

Proto-Neutron and Neutron Stars in a Chiral SU(3) Model

V. Dexheimer and S. Schramm

*Frankfurt Institute for Advanced Studies
Johann Wolfgang Goethe University
Ruth-Moufang-Str. 1, 60438 Frankfurt am Main, Germany.*

dexheimer@th.physik.uni-frankfurt.de

ABSTRACT

A hadronic chiral SU(3) model is applied to neutron and proto-neutron stars, taking into account trapped neutrinos, finite temperature and entropy. The transition to the chirally restored phase is studied and global properties of the stars like minimum and maximum masses and radii are calculated for different cases. In addition, the effects of rotation on neutron star masses are included and the conservation of baryon number and angular momentum determine the maximum frequencies of rotation during the cooling.

Subject headings: neutron stars, proto-neutron stars, chiral restoration, star cooling, star rotation

1. Introduction

After a core-collapse supernova explosion of a star with a mass smaller than about 20 solar masses, the remaining star, initially called proto-neutron star, is left with a very high temperature of up to 50 MeV. Due to their short mean free path especially electron neutrinos stay trapped for roughly 10 to 20 seconds and develop a finite chemical potential. In this stage the structure of the star can be divided into a core region that will be modelled in this article, and an envelope with higher entropy. Maximum and minimum star masses as well as rotational constraints on them will be considered. Finally, the corresponding properties of the cooled neutron star will be determined as well.

As a direct solution of the QCD equations for a high-density hadronic environment is currently out of reach, the core region of the star will be described using an effective SU(3) chiral model including hyperonic degrees of freedom. The effect of strange hadrons on the properties of neutron stars has been discussed in the past by a number of authors including

the investigation of kaon condensation (Kaplan et al. (1986); Pons et al. (2000)) and studies of the effect of hyperons in neutron stars (Glendenning et al. (1991, 2001); Jha et al. (2006, 2007)) and references in Page et al. (2006)). Here in a general approach the baryons and mesonic fields are introduced as flavor-SU(3) multiplets. The baryons obtain their masses through their coupling to the scalar meson fields via spontaneous symmetry breaking. The parameters of the theory are fixed to reproduce the hadronic vacuum masses as well as the properties of ground state nuclear matter. The model is extended to include effects from the lowest spin-3/2 baryonic multiplet. The model has been successfully applied to the description of nuclear matter and finite nuclei (Papazoglou et al. (1998, 1999)) as well as to the high-temperature and high-density environment of an ultrarelativistic heavy-ion collision (Zschesche et al. (2007)). A study of neutron stars had also been performed (Hanauske et al. (1999); Schramm et al. (2003)). In the following these calculations are extended to proto-neutron star environments with finite temperature and neutrino chemical potential, additionally considering the population of higher baryonic resonances. In a further refitting of the basic model parameters, a study of the maximally achievable star masses in this approach is presented, while still maintaining a phenomenologically reasonable description of ground state nuclear matter.

The article is organized as follows. In section 2 the hadronic degrees of freedom and the model Lagrangian will be briefly presented. In section 3 the model will be applied to zero-temperature neutron stars with special emphasis on the effect of non-linear meson interactions. The properties of proto-neutron stars at finite temperature, entropy and lepton number are shown and discussed in section 4. Finally, the effects of rotation and its consequences on the cooling of the star are analyzed and conclusions are presented.

2. The Hadronic Model

Since in a high-density environment like the one present in the center of neutron stars the baryonic chemical potential is high enough to create particles beyond the lowest SU(2) multiplet of the nucleons, which comprise hyperons (Λ , Σ , Ξ) and possibly other resonance states (Δ , Σ^* , Ξ^* , Ω), the hadronic model is based on a flavor-SU(3) description including hyperons and strange mesons as part of the basic hadronic SU(3) multiplets, which were also partially taken into account in previous works (Schaffner et al. (1996); Jha et al. (2007)). The baryons interact via exchange of scalar (σ , δ , ζ , χ) and vector mesons (ρ , ω , ϕ). The isovector vector (ρ) and scalar (δ) mesons are included in a natural way, as an essential ingredient for reproducing the phenomenological value for the asymmetry energy of nuclear matter. A scalar isoscalar (dilaton) field (χ) acts as an effective gluon condensate. On the

leptonic side, electrons and muons assure charge neutrality and neutrinos are considered in the case of proto-neutron stars.

The Lagrangian density of the chiral model in mean field approximation used in our calculations reads:

$$L_{MFT} = L_{Kin} + L_{Bscal} + L_{Bvec} + L_{scal} + L_{vec} + L_{SB}, \quad (1)$$

where besides the kinetic energy term for baryons and leptons, the terms:

$$L_{Bscal} + L_{Bvec} = - \sum_i \bar{\psi}_i [g_{i\omega} \gamma_0 \omega + g_{i\phi} \gamma_0 \phi + g_{i\rho} \gamma_0 \tau_3 \rho + m_i^*] \psi_i, \quad (2)$$

$$L_{vec} = -\frac{1}{2}(m_\omega^2 \omega^2 + m_\rho^2 \rho^2 + m_\phi^2 \phi^2) \frac{\chi^2}{\chi_0^2} + L_{vec,4}, \quad (3)$$

$$\begin{aligned} L_{scal} = & \frac{1}{2} k_0 \chi^2 (\sigma^2 + \zeta^2 + \delta^2) - k_1 (\sigma^2 + \zeta^2 + \delta^2)^2 \\ & - k_2 \left(\frac{\sigma^4}{2} + \frac{\delta^4}{2} + 3\sigma^2 \delta^2 + \zeta^4 \right) - k_3 \chi (\sigma^2 - \delta^2) \zeta \\ & + k_4 \chi^4 + \frac{1}{4} \chi^4 \ln \frac{\chi^4}{\chi_0^4} - \epsilon \chi^4 \ln \frac{(\sigma^2 - \delta^2) \zeta}{\sigma_0^2 \zeta_0}, \end{aligned} \quad (4)$$

$$L_{SB} = \left(\frac{\chi}{\chi_0} \right)^2 \left[m_\pi^2 f_\pi \sigma + \left(\sqrt{2} m_k^2 f_k - \frac{1}{\sqrt{2}} m_\pi^2 f_\pi \right) \zeta \right], \quad (5)$$

represent the interactions between baryons and scalar mesons and between baryons and vector mesons, the self interactions of scalar and vector mesons and an explicitly chiral symmetry breaking term, responsible for producing the masses of the pseudo-scalar mesons. In Eqs. (2-5) the mesons are treated as classical fields within the mean-field approximation. Only the 0th component of the vector meson survives, i.e. $\omega \equiv \omega_0$, $\rho \equiv \rho_0^0$, $\phi \equiv \phi_0$. σ and ζ are the scalar fields corresponding to the non-strange and strange quark condensate, respectively. A detailed discussion of this Lagrangian can be found in Papazoglou et al. (1998, 1999). The baryon masses are generated by the scalar fields except for a small explicit mass term equal to $\delta m \sim 150$ MeV for nucleons. The effective masses decrease at high densities with decreasing scalar fields as the chiral symmetry is partially restored. At low densities they reproduce the experimentally known baryon masses:

$$m^* = g_{i\sigma} \sigma + g_{i\delta} \tau_3 \delta + g_{i\zeta} \zeta + \delta m. \quad (6)$$

The coupling constants used to calculate proto-neutron star properties ($g_{N\omega} = 11.9$, $g_{N\phi} = 0$, $g_{N\rho} = 4.03$, $g_{N\sigma} = -9.83$, $g_{N\delta} = -2.34$, $g_{N\zeta} = 1.22$, $k_0 = 2.37$, $k_1 = 1.40$, $k_2 = -5.55$, $k_3 = -2.65$, $k_4 = -0.23$, $\epsilon = 0.06$, $g_4 = 38.9$) are chosen to reproduce the vacuum

masses of the baryons and mesons, the nuclear saturation properties (density $\rho_B = 0.15\text{fm}^{-3}$, binding energy per nucleon $B/A = -16.00$ MeV, compressibility $K = 297.32$ MeV), the asymmetry energy ($E_{sym} = 32.50$ MeV), and reasonable values for the hyperon potentials ($U_\Lambda = -29.41$ MeV, $U_\Sigma = 20.39$ MeV, $U_\Xi = -10.09$ MeV). The vacuum expectation values of the scalar mesons are constrained by reproducing the pion and kaon decay constants.

3. Neutron Stars

In the calculation of zero-temperature neutron stars the influence of the structure of the self interaction term of the vector mesons is investigated, as in dense systems baryonic vector densities, and therewith the mean fields of the vector mesons, become especially important for the equation of state of hadronic matter. The fourth-order self-interaction term $L_{vec,4}$ of the vector mesons can be written in different forms in a SU(3)-invariant way. To study the difference in the result three separate coupling schemes are considered,

$$L_{vec,4} = -g_4[Tr(V)]^4/4 \quad (a), \quad -g_4[Tr(V^2)]^2 \quad (b), \quad -g_4 2Tr(V^4) \quad (c) \quad , \quad (7)$$

where V stands for the 3x3 matrix of the vector meson multiplet, which reduces to a diagonal form in the mean field limit, i. e. $V = ((\omega + \rho)/\sqrt{2}, (\omega - \rho)/\sqrt{2}, \phi)$. The mass-radius relation of the respective neutron star for the cases (a) to (c) was calculated by solving the Tolman-Oppenheimer-Volkov (TOV) equations for static spherical stars (Tolman (1939); Oppenheimer et al. (1939)). The results are shown in Fig. 1 in the SU(2) limit of proton, neutron and electron matter. A strong coupling of the ω and ρ meson present in the cases (b) and (c) leads to smaller star masses. In the following calculations the non-linear coupling (a), which does not generate a $\rho - \omega$ coupling, is used. This allows for more massive neutron stars and is also in general agreement with the observed small mixing of the two mesons.

The modification of the original parameter set C1 of the model, used in Papazoglou et al. (1999) was done in order to investigate the maximum neutron star masses that can be achieved in the model (similar studies in a different approach have been done in Jha et al. (2007)), while still reproducing the hadronic masses in the vacuum as well as reproducing the phenomenological values of the basic nuclear matter ground state properties as listed in the previous section. Within the model different situations can be analyzed by including the whole baryon octet or, in addition, the baryon decuplet. In practice, the only baryons present in the star besides the nucleons are the Λ and Σ^- in the first case (Fig. 2) and Λ , $\Delta^{-0,+,+}$, in the second case (Fig. 3). In the presence of resonances the Δ^- particle replaces the Σ^- , as its effective mass drops faster with density compared to the Σ^- . As can be seen from Fig. 4 the inclusion of new particles, i.e. new degrees of freedom, softens the equation

of state (EOS). The same effect would be observed in the symmetric case, when there is no net isospin instead of no net electric charge, in the presence of more massive degrees of freedom. Although the symmetric case has no relevance for neutron stars due to their high intrinsic asymmetry this case is important for example in heavy ion collisions.

The softening of the equation of state causes a decrease of the respective neutron star maximum mass (Fig. 5). Besides using the high density EOS for the interior of the star, in order to calculate the mass-radius diagram, an inner crust, an outer crust and an atmosphere have been considered following Baym et al. (1971). The studies of the proto-neutron star properties are restricted to the model including the lowest multiplets, i.e. including the baryon octet, thus avoiding the uncertainties related to the largely unknown coupling strengths of the baryonic decuplet. In this case, it is possible to describe stars with masses higher than $M = 2M_\odot$ and still take into account heavy baryonic degrees of freedom.

The transition to the chirally restored phase for any of the considered self-interactions and sets of baryonic degrees of freedom turns out to be a cross over. This happens due to the requirements of beta equilibrium and charge neutrality that make the different isospin states of baryons with the same vacuum mass appear at different densities of the star, thus smoothing out their effect. This transition can be seen in the behavior of the scalar condensate σ used here as the order parameter for the transition. In Fig. 6 the condensate was plotted against the star radius showing that in this model the chiral symmetry is partially restored in neutron stars.

4. Proto-Neutron Stars

Right after the supernova explosion, due to the neutronization of the matter, the star contains an abundant number of neutrinos that are trapped in the system. The temperature of the star can reach values of up to 50 MeV. In order to determine the matter properties under these conditions the thermodynamical potential of the grand canonical ensemble is solved. It is defined as:

$$\frac{\Omega}{V} = -L_{scal} - L_{vec} - L_{SB} - L_{vac} \mp T \sum_i \frac{\gamma_i}{(2\pi)^3} \int_0^{k_{F_i}} d^3k \ln(1 \pm e^{-\frac{1}{T}(E_i^*(k) - \mu_i^*)}), \quad (8)$$

where i denotes the fermion type (including leptons), γ_i the fermionic degeneracy, $E_i^*(k) = \sqrt{k^2 + m_i^{*2}}$ the energy, and $\mu_i^* = \mu_i - g_\omega \omega_0 - g_\rho \rho_{03} \tau_3 / 2 - g_\phi \phi_0$ the effective chemical potential (a vanishing chemical potential for muon neutrinos has been assumed here). In the case of leptons $m^* = m$ and $\mu^* = \mu$. The single particle energy is given by $E_i(k) = E_i^*(k) +$

$g_\omega\omega + g_\rho\rho\tau_3/2 + g_\phi\phi$ and the entropy per volume per baryon is defined as $s = S/V/\rho_B = -d\Omega/dT|_{V,\mu}/\rho_B$.

To study this complex system two different features are taken into account separately: finite temperature and high lepton number. In a static approximation of the evolution of the star three different approaches are considered as they have appeared in the literature:

- constant temperature: in this case the whole star is considered at the same temperature, which is unrealistic, and the maximum mass of the star is higher for higher temperatures because of the thermal effects on the binding part of the mass. In this case the entropy per baryon remains constant with the increase of density except for small densities as can be seen in Fig. 7. This effect comes from the fact that even when the baryon density tends to zero, the electron-positron pairs present at finite temperature still contribute for the entropy. The transition to the chirally restored phase becomes smoother with the increase of temperature since the Fermi surface becomes less important (Fig. 8).
- metric dependent temperature: in this case, as discussed in Gondek et al. (1997), the temperature is defined at an infinite distance from the star and the thus defined temperature increases as the gravitational field created by the presence of the star mass becomes higher: $T = T_\infty/\sqrt{g_{00}}$, where g_{00} is the 00 component of the metric tensor. As the gravitational field increases toward the center of the star the density also increases as can be seen in Fig. 9 for $T_\infty = 15$ MeV, but the increase of the temperature from the center to the edge of the star is not too pronounced. In this case, the maximum mass of the star is higher for higher temperatures T_∞ .
- constant entropy: in this case the star is considered to have a constant entropy throughout, which to some degree agrees with dynamical simulations of the stellar evolution (Stein et al. (2006)). The temperature is higher in the center of the star and colder at the edge as can be seen in Fig. 10 and the maximum mass of the star is higher for higher entropies also because of the thermal effects on the binding part of the mass.

The trapped neutrinos with a chemical potential μ_ν are included by fixing the lepton number defined as $Y_l = (\rho_e + \rho_{\nu_e})/\rho_B$. In consequence there will be a large number of neutrinos in the star but also an increased electron density. Therefore, demanding charge neutrality, the proton density increases, and with higher proton density, the star becomes more isospin symmetric and the neutron Fermi energy decreases. Thus the increase of lepton number softens the EOS and consequently the maximum mass of the neutron star gets smaller. It is important to keep in mind that this result is dependent on the chosen

parameter set and consequently on the particles present in the star. For parameter sets that allow the hyperons to appear at lower densities, the high proton density delays their population allowing the neutron star to be more massive.

These two features can be put together to describe the evolution of the star for the extreme cases: constant temperature and fast increasing temperature throughout the star. After the supernova explosion, the star is still warm so the temperature is fixed to $T = 30$ MeV or the entropy per baryon is fixed to $s = 2$ (the temperature increases from 0 at the edge up to 50 MeV in the center as in Fig.10). The star still contains a high abundance of neutrinos that were trapped during the explosion so the lepton number is fixed to a typical value of $Y_l = 0.4$. After several seconds (10-20) the neutrinos escape and β -equilibrium is established. After about a minute, the temperature of the star has dropped below 1 MeV.

The balance between the effects of temperature/entropy and lepton number is very delicate and depends on the parameters of the model. The first line in table 1 shows the maximum star masses for different entropies and different temperatures. As can also be seen in Figs. 11 and 12 the intermediate step of the evolution with $s = 2$ and $\mu_\nu = 0$ is more massive than the first one. But this calculation does not take into account that the baryon number does not increase as the star gets colder, otherwise it would collapse into a black hole (Takatsuka et al. (1995)). If the baryon number is fixed starting with the values for the star with $s = 2$ or $T = 30$ MeV, resp., and $Y_l = 0.4$, the stable solutions of the colder cases have a smaller mass than the warmer case as can be seen in the second line of Tab. 1.

In stars with finite temperature/entropy a crust of high entropy has been used since the shock wave created during the supernova explosion leaves the outer region with a much higher entropy than the rest of the star and it remains warmer for longer time serving as an insulating blanket, which delays the star from coming to a complete thermal equilibrium with the interstellar medium (Lattimer et al. (1991)). In this case the crust is stiff enough to generate massive stars for small central energies resulting in big radii. Because of the use of a warm crust it is also possible to stipulate a minimum mass for each case (fourth line of Tab. 1). For the assumption of constant temperature the crust used has an entropy $s = 5$ so that the inner and outer EOS could be continuously connected but as a result the minimum mass found is far from a realistic value ($M \sim 1.18M_\odot$, Faulkner et al. (2004)). For the constant entropy case the crust used has a value of $s = 4$.

5. Rotation

As the proto-neutron star cools down, its possible radii and masses change (Tab. 1), which means that its moment of inertia changes and for determining the maximum frequency of the star one has to take into account angular momentum conservation (Takatsuka et al. (1995)). The maximum frequency (Kepler frequency) with which a star can rotate without starting to expel matter on the equator, has been determined by including monopole and quadrupole corrections to the metric due to the rotation and solving the self-consistency equation for Ω_K as it was derived in Glendenning et al. (1994). In the current calculations rotational instabilities, that would potentially reduce the maximum rotational frequency, are not taken into account. The rotation of the star generates a modification of the metric and the higher the rotational frequency, the higher the mass and radius of the star become (Schramm et al. (2003)) as can be seen in Fig. 13. The maximum masses calculated in this approximation differ by less than 1% from full calculation results (Stergioulas et al. (1995)) for frequencies around 716 Hz. For this set of parameters the increase in the maximum masses of the stars from $\nu = 0$ to $\nu = \nu_K$, fixing the baryon number to the value for zero frequency, is smaller than 5%, different from the 15% mass increase in the case that the baryon number is not fixed. But this situation can be identified as the spin down of a cold star with a certain baryon number (in this case 0.28×10^{58} N) that continues until it emits all its energy and stops rotating. In this point the star is considered dead.

To consider the rotational effects in the cooling from the very first stage of the neutron star life, besides the baryon number, the angular momentum has to be taken into account since it remains about constant in the first seconds of the cooling. This new constraint lowers even more the possible maximum mass and Kepler frequency of the star as can be seen in Tab. 2. As a consequence of that, some stars are stable during a stage of cooling but not in the subsequent one, causing matter to be lost during the process.

6. Conclusion

For the first time an effective model including hyperon degrees of freedom could generate a neutron star with a mass $M \sim 2.1 M_o$ in agreement with the most massive one observed but still under discussion (Nice et al. (2005)). The inclusion the baryonic spin-3/2 multiplet as additional degrees of freedom still leads to a quite heavy star of about 1.9 solar masses. This mass might be lowered when the cooling process of the star is examined and the baryon number is fixed in the early stage of the proto-neutron star life. The maximum mass of the star increases again when rotation is included to values beyond $M = 2.0M_o$ for a frequency of $\nu = 1122\text{Hz}$, the highest frequency measured for pulsars so far (Kaaret et al. (2007)) but

because of the baryon number and angular momentum constraints, a range of masses in fast rotating stars leads to unstable states and shedding of matter.

The transition to a largely chirally restored phase takes place in the core of the neutron star within the chiral model, although for all scenarios that were considered here, the restoration occurs via a smooth cross over due to the requirements of beta equilibrium and charge neutrality.

7. Acknowledgements

We thank Horst Stöcker for valuable discussions and suggestions. V. D. acknowledges the financial support of the Josef-Buchmann-Stiftung. Part of the numerical work has been done on the facilities of the Center for Scientific Computing, University of Frankfurt.

REFERENCES

- D. B. Kaplan and A. E. Nelson, *Phys. Lett. B* **175**, 57 (1986).
- J. A. Pons, S. Reddy, P. J. Ellis, M. Prakash, and J. M. Lattimer, *Phys. Rev. C* **62**, 035803 (2000)
- N. K. Glendenning and S. A. Moszkowski, *Phys. Rev. Lett.* **67**, 2414 (1991)
- N. K. Glendenning, *Phys. Rev. C* **64**, 025801 (2001)
- T. K. Jha, P. K. Raina, P. K. Panda, and S. K. Patra, *Phys. Rev. C* **74**, 055803 (2006)
- T. K. Jha, H. Mishra and V. Sreekanth, arXiv:0710.5392 [nucl-th].
- D. Page and S. Reddy, *Ann. Rev. Nucl. and Part. Sci.*, **56**, 327 (2006).
- P. Papazoglou, S. Schramm, J. Schaffner-Bielich, H. Stoecker and W. Greiner, *Phys. Rev. C* **57**, 2576 (1998).
- P. Papazoglou, D. Zschesche, S. Schramm, J. Schaffner-Bielich, H. Stoecker and W. Greiner, *Phys. Rev. C* **59**, 411 (1999).
- D. Zschesche, G. Zeeb and S. Schramm, *J. Phys. G* **34**, 1665 (2007).
- M. Hanauske, D. Zschesche, S. Pal, S. Schramm, H. Stoecker and W. Greiner, arXiv:astro-ph/9909052.

- S. Schramm and D. Zschiesche, *J. Phys. G* **29**, 531 (2003).
- J. Schaffner and I. N. Mishustin, *Phys. Rev. C* **53**, 1416 (1996).
- R. C. Tolman, *Phys. Rev.* **55**, 364 (1939).
- J. R. Oppenheimer and G. M. Volkoff, *Phys. Rev.* **55**, 374 (1939).
- G. Baym, C. Pethick and P. Sutherland, *Astrophys. J.* **170**, 299 (1971).
- D. Gondek, P. Haensel and J. L. Zdunik, *Astron. Astrophys.* **325**, 217 (1997).
- J. Stein and J. C. Wheeler, *Astrophys. J.* **643**, 1190 (2006).
- T. Takatsuka, *Nucl. Phys. A* **588**, 365 (1995).
- J. M. Lattimer and F. D. westy, *Nucl. Phys. A* **535**, 331 (1991).
- A. J. Faulkner *et al.*, *Astrophys. J.* **618**, L119 (2004).
- N. K. Glendenning and F. Weber, *Phys. Rev. D* **50**, 3836 (1994).
- N. Stergioulas and J. L. Friedman, *Astrophys. J.* **444**, 306 (1995)
- D. J. Nice, E. M. Splaver, I. H. Stairs, O. Loehmer, A. Jessner, M. Kramer and J. M. Cordes,
Astrophys. J. **634**, 1242 (2005).
- P. Kaaret *et al.*, arXiv:astro-ph/0611716.

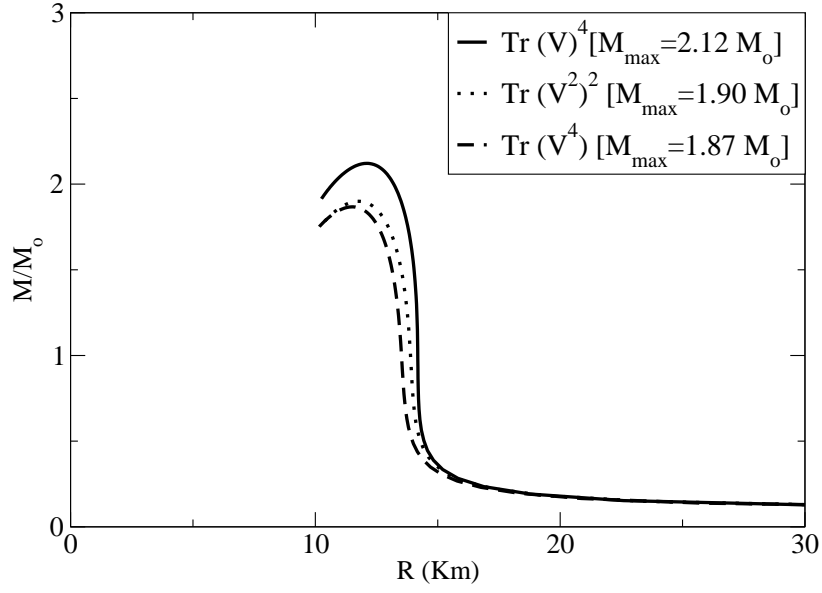


Fig. 1.— Star mass versus radius for different vector meson self interactions.

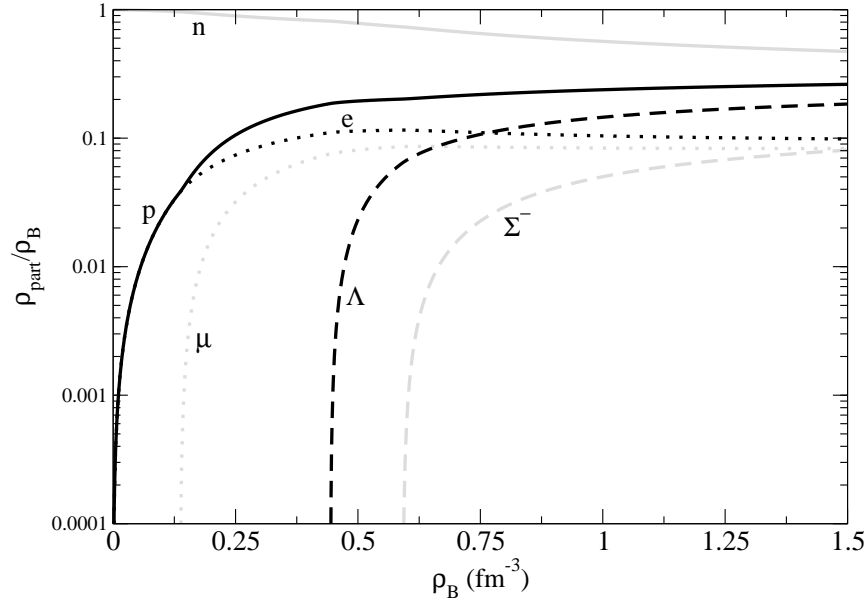


Fig. 2.— The composition of neutron star matter with hyperons.

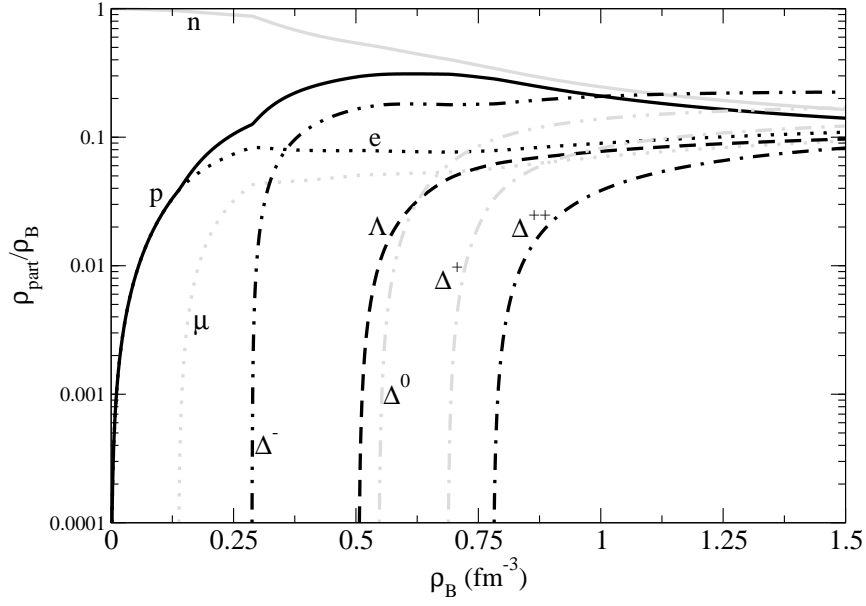


Fig. 3.— The composition of neutron star matter with hyperons and resonances.

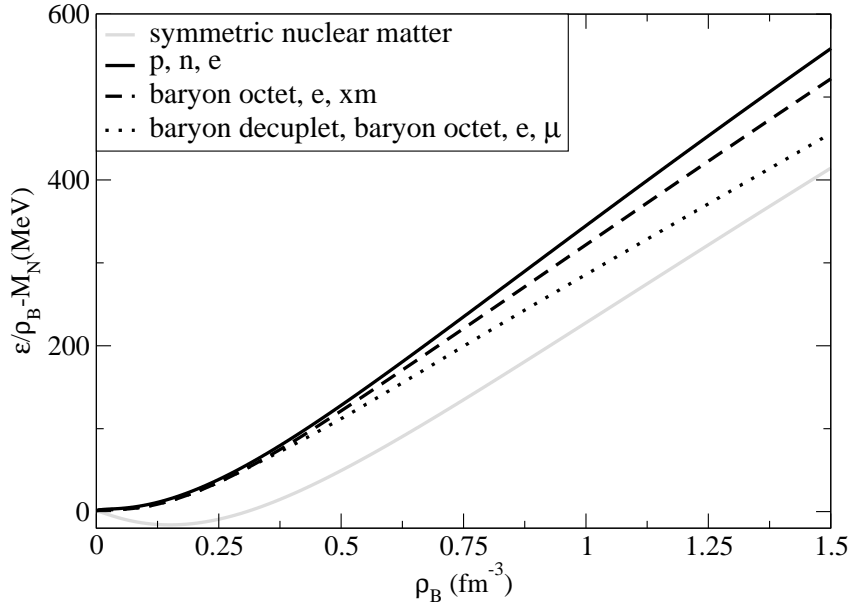


Fig. 4.— Binding energy per nucleon versus baryon density.

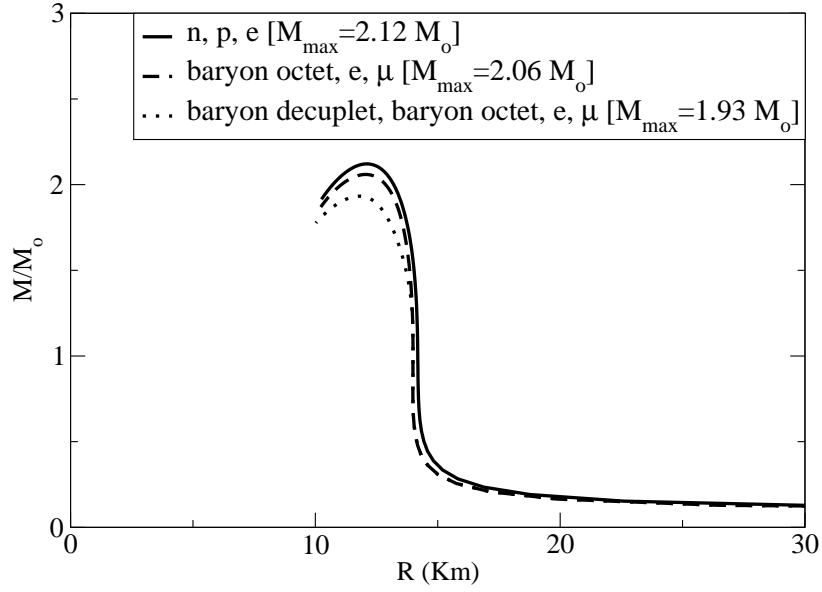


Fig. 5.— Star mass versus radius for different compositions.

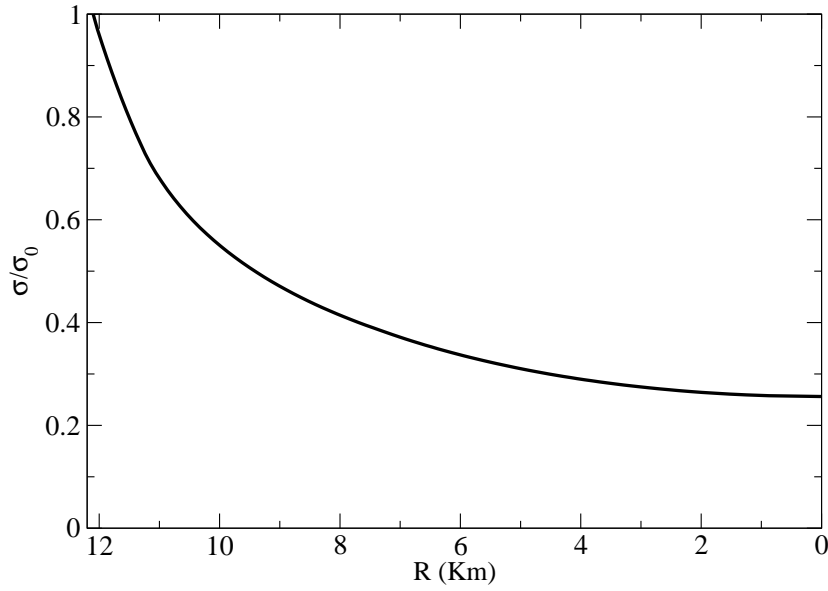


Fig. 6.— Scalar condensate versus star radius.

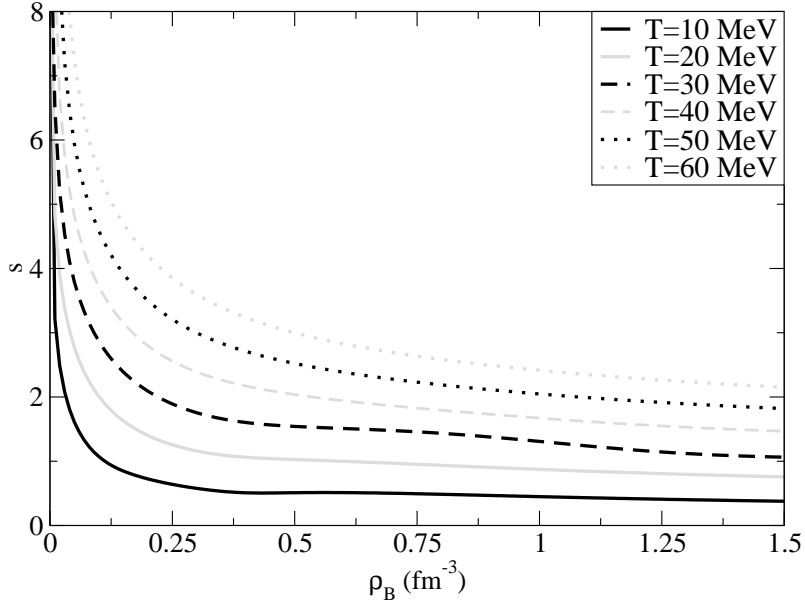


Fig. 7.— Entropy per volume per baryon versus baryon density for different temperatures.

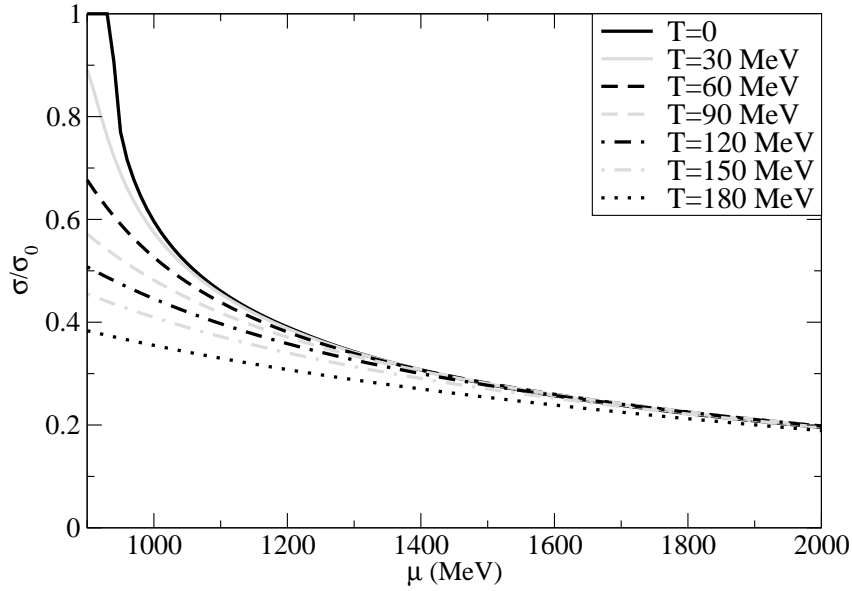


Fig. 8.— Scalar condensate versus chemical potential for different temperatures.

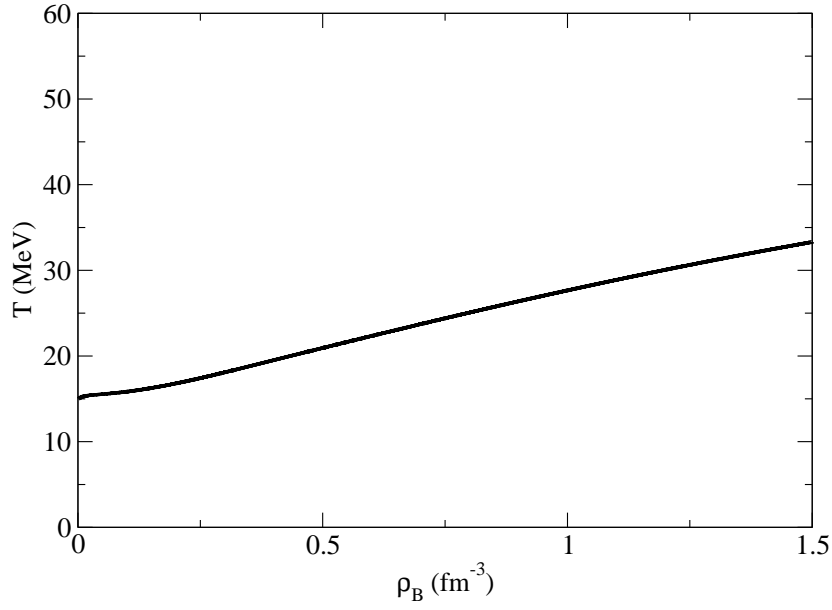


Fig. 9.— Temperature versus baryon density for $T_\infty = 15$ MeV.

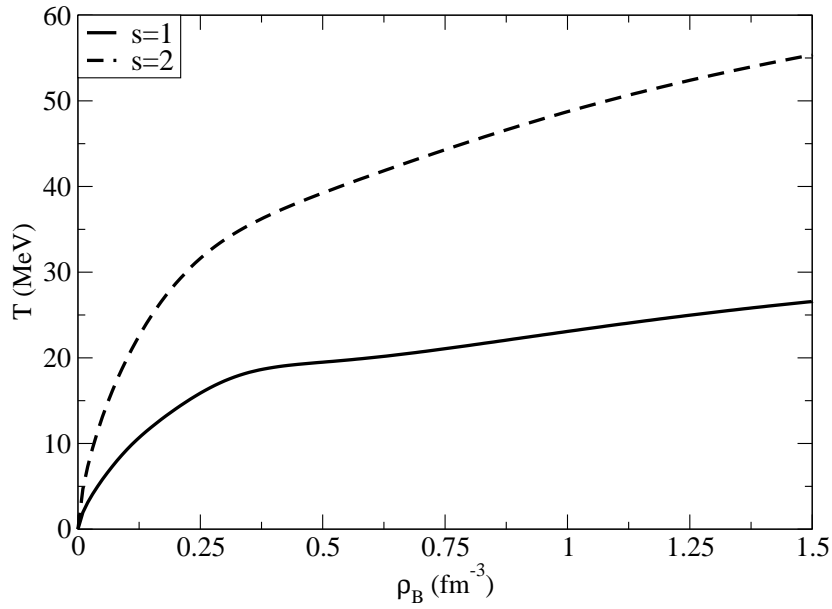


Fig. 10.— Temperature versus baryon density for different entropies per volume per baryon.

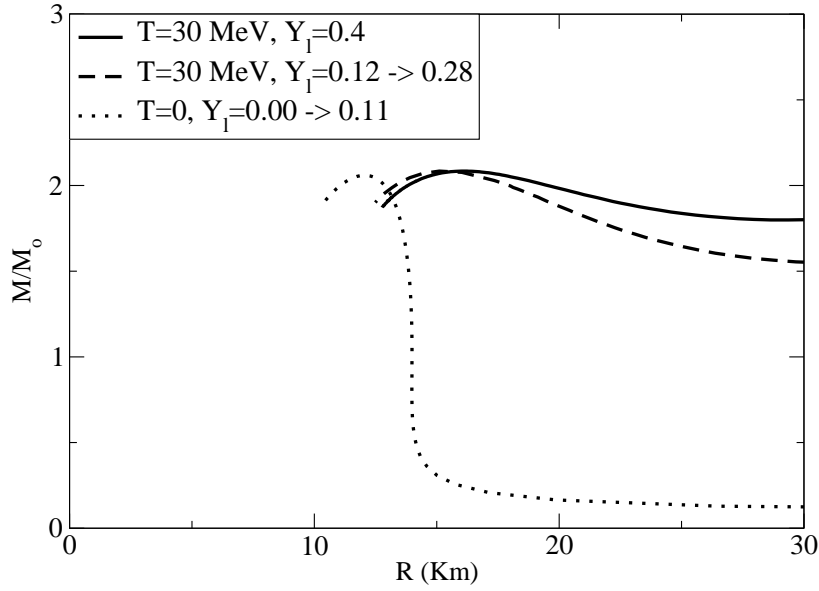


Fig. 11.— Star mass versus radius for different moments of the star evolution defined by temperature and lepton number considering the baryon octet, e , μ .

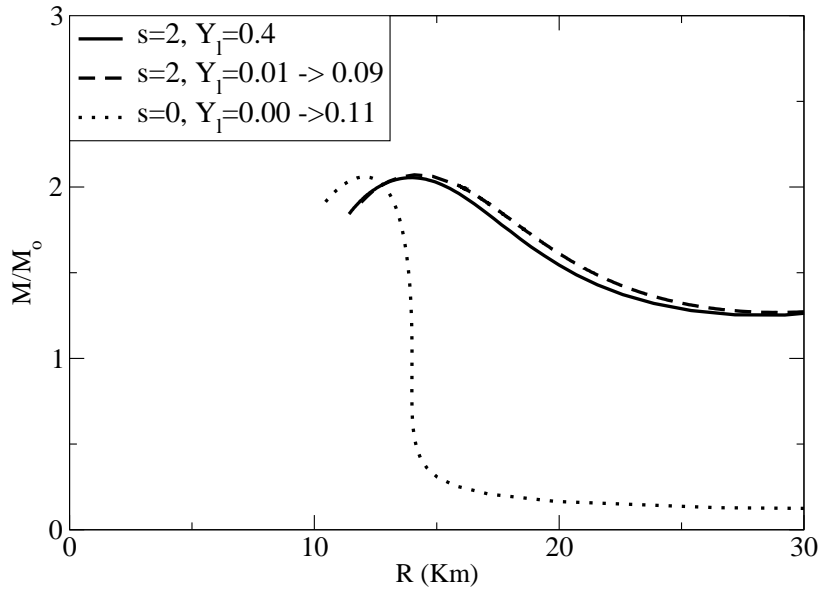


Fig. 12.— Star mass versus radius for different moments of the star evolution defined by entropy and lepton number considering the baryon octet, e , μ .

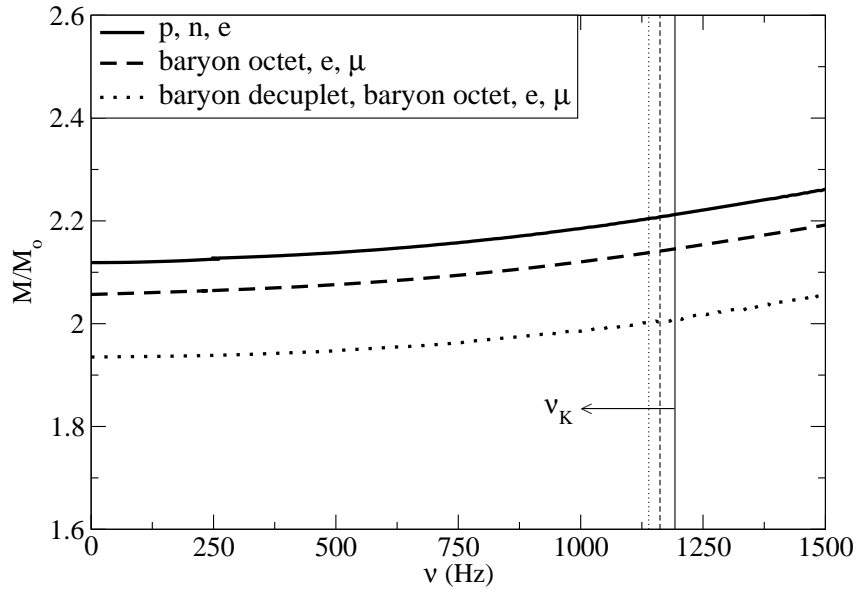


Fig. 13.— Star mass versus rotational frequency of the star for different compositions.

Table 1: Maximum masses with and without fixing the baryon number, radii for the maximum masses with fixed baryon number and minimum masses with and without fixing the baryon number for different moments of the star evolution.

stages	$s = 2$	$s = 2$	$s = 0$	$T = 30$ MeV	$T = 30$ MeV	$T = 0$ MeV
	$Y_l = 0.4$	β equil.	β equil.	$Y_l = 0.4$	β equil.	β equil.
$M_{max}(M_o)$	2.05	2.07	2.05	2.08	2.08	2.05
fixed M_B	2.05	2.01	1.96	2.08	2.03	1.99
$R(km)$	14.00	15.87	12.44	16.09	17.23	12.33
$M_{min}(M_o)$	1.07	1.07	0.02	2.02	2.02	0.02
fixed M_B	1.07	1.07	0.94	2.02	2.02	1.77

Table 2: Maximum frequencies and masses with and without fixing M_B and L for different stages of the cooling.

stages	$s = 2, Y_l = 0.4$	$s = 2, \beta$ equil.	$s = 0, \beta$ equil.	$s = 0, \beta$ equil.
$\nu_K(Hz)$	1452.56	1424.48	1515.86	0
$M_{max}(M_o)$	2.31	2.33	2.34	2.06
fixed M_B	1228.23	1110.28	1162.03	0
	2.25	2.19	2.14	2.06
fixed L	1195.30	1095.90	1162.03	
	2.24	2.19	2.14	